

INTERMODULATION DISTORTION IN MICROWAVE MESFET AMPLIFIERS

Ramesh K. Gupta, Colin G. Englefield, Paul A. Goud
Department of Electrical Engineering
The University of Alberta
Edmonton, Alberta T6G 2G7 Canada

ABSTRACT

The third-order intermodulation distortion (IM_3) of a MESFET amplifier has been analysed using Volterra series representation. A model is described that takes into account the MESFET nonlinearities and their interaction with the surrounding microwave circuit. A theoretical and experimental study of the amplifier intermodulation products has been conducted. Their dependence on the input frequency and power-level of a two-tone test signal is investigated. For power inputs less than -10 dBm, the agreement obtained between measured and predicted IM_3 is within 3-dB over an amplifier bandwidth of 400 MHz.

Introduction

The intermodulation distortion of microwave MESFET amplifiers is an important characteristic affecting their use in multi-carrier telecommunication systems. In this paper, the third-order intermodulation performance of a GaAs MESFET amplifier is investigated. The Volterra series representation is used as the analysis technique. A lumped-circuit model of the amplifier, that takes into account the device non-linearities and their interaction with the embedding microwave circuitry, is described. A large-signal model of the transistor is obtained from the bias and frequency dependence of the measured small-signal device S-parameters. This modelling technique has previously been used for predicting the large-signal performance of MESFETs, mounted in a 50 Ω system [1, 2]. Our analysis is directed towards a more practical problem, where the device sees frequency-dependent impedances.

Device Characterisation

An accurate in-situ characterisation procedure for the device was realised by first characterising the transistor fixture. The discontinuities and losses associated with the input and output coaxial connectors and the coaxial-to-microstrip transitions were modelled by measuring the two-port S-parameters over a discrete set of frequencies, with a 50-ohm line between the connectors. Measurements were made both with and without D.C. blocking capacitors. The computer program COMPACT [3] was used to optimise the circuit parameters of the model. The circuit topology for these discontinuities and losses is shown in Fig. 1(a). An HP HFET-1101 GaAs FET was mounted in the fixture, in the common source configuration, and the composite S-parameters were measured for different transistor bias conditions. The gate-to-source voltage V_{GS} required for total pinch-off of the transistor was measured to be -2V. The characterisation was carried out for several values of V_{GS} and drain-to-source voltage V_{DS} . An error-correction procedure was used to correct for the errors associated with the imperfections of the network analyzer. A lumped-circuit device model, that included the effect of feedback elements such as drain-to-gate capacitance C_{dg} and source lead resistance R_s and inductance L_s , was used (see Fig. 1(b)). This device model with the modelled fixture parameters was least-square fitted to the measured composite S-parameters. The linear elements of the composite model were kept fixed, and the bias dependence of the non-linear elements was computed. These non-linear elements are the gate-to-source capacitance C_{gs} , the transconductance g_m , drain-to-gate capacitance C_{dg} and output resistance R_o . The modelled device parameter values, for $V_{DS}=3.0V$ and $V_{GS}=-1.0V$ are listed in Table 1.

Amplifier Design and Performance

The amplifier matching circuits were designed using de-embedded S-parameters of the transistor, for $V_{DS}=3.0V$ and $V_{GS}=-1.0V$. The amplifier was constructed using open microstrip circuitry, with Epsilam 10 substrate material ($\epsilon_r=10.2$). The amplifier was observed to have a small-signal gain of 9.2 dB at a centre frequency of 6.1 GHz for $V_{DS}=3.0V$ and $V_{GS}=-1.0V$. As the gate voltage is made more negative, the gain of the amplifier decreases and the bandwidth increases. The family of curves representing the measured and modelled small-signal gain of the amplifier is plotted in Fig. 2. The agreement obtained in magnitude and phase is within 1 dB and 30 degrees, respectively. The amplifier was predicted to be unstable for $V_{GS}=-0.1V$, $V_{DS}=3.0V$; therefore the operation of the amplifier was restricted to gate voltage levels below $V_{GS}=-0.5V$. Good agreement was obtained between the measured and the modelled amplifier response over a frequency range from 4.8 GHz to 7.2 GHz.

Device Nonlinearities

The bias dependence of the nonlinear circuit elements of the FET was observed to be similar to that expected from device physics relationships. R_o was observed to be almost constant as a function of gate voltage over the operating range of interest, but linearly dependent on the drain voltage, V_{DS} . Since the output resistance is not directly a part of the FET gain mechanism its contribution to the intermodulation distortion will be small. An averaged value of R_o was therefore used. Further, an averaged value of time delay τ_o associated with g_m can be used without much loss of accuracy [2]. The analytical expressions for the nonlinear device parameters g_m and C_{gs} [4] were curve-fitted to the measured data. A comparison of their modelled and measured parameter values is shown in Figs. 3(a) and 3(b). Since no simple relationship is available to model the dependence of C_{dg} on V_{DG} , an empirical relationship was curve-fitted to the measured data.

The modelled expressions for C_{gs} , g_m and C_{dg} were expanded into a power series and the nonlinear coefficients were obtained. Since the nonlinearities are small, the series is truncated after three terms. For amplifiers with less than an octave bandwidth, such as the FET amplifier considered here, even-order terms produce distortion products which fall outside the amplifier band [5]. Therefore, the second-order terms were ignored. The third-order nonlinear coefficients for $V_{DS}=3.0V$ and $V_{GS}=-1.0V$ were computed to be $C_{gs3}=0.01422$ $pF|V^2$, $g_{m3}=-1.2817$ m mho $|V^2$ and $C_{gd3}=0.00190$ $pF|V^2$.

Non-linear Model and Volterra Series Analysis

Fig. 1(b) depicts the lumped circuit model for the amplifier used for the Volterra series analysis. P_a and Q_a refer to the external ports of the amplifier while P_d and Q_d are the device ports. The distributed circuit between these two reference ports consists of the matching circuits, the coaxial-to-microstrip transitions, D.C. blocking capacitors and coaxial connectors. (see Fig. 1(a)). $Z_s(\omega)$ and $Z_L(\omega)$ are the source and the load impedances as seen from the device gate and drain ports P_d and Q_d , respectively. \hat{i}_C , \hat{i}_{g_m} and $\hat{i}_{C_{dg}}$ represent the small nonlinear distortion currents which are superimposed upon the linear circuit currents. Six nodes are defined for the overall amplifier circuit. v_1^+ , i_1^+ , and v_1^- , i_1^- are the equivalent voltage and current components of the incident and reflected waves at node 1. i_1 represents the net current flowing into the gate circuit of the transistor and v_1 is the terminal voltage at node 1. v_6^+ , i_6^+ , v_6^- , i_6^- and v_6 , i_6 refer to the corresponding voltages and currents at node 6. These voltages and currents are related to the input and the output power, at ports P_a and Q_a of the amplifier, through simple relationships.

A set of nodal equations is derived for the overall circuit by applying Kirchoff's current law to the terminal currents and voltages at each node. Nonlinear distortion currents are included as voltage and frequency-dependent current sources. Each nodal voltage is expressed by a Volterra series expansion of the incident voltage. Narayanan's approach [6] is used to determine the nodal voltage Volterra kernels. The second degree kernels are identically zero, since the second degree terms of the expansions have been ignored. The linear kernels and the third-degree were numerically computed. The third-order intermodulation distortion performance of the MESFET amplifier was investigated as a function of frequency, input power level of a two-tone test signal, and different gate bias voltages of the transistor.

The experimental results were obtained by applying a two-tone signal at the input of the amplifier. The two tones were kept 1 MHz apart by locking the two microwave sources through a phase-locked loop circuit. The power output for the fundamental component of the output signal, and the distortion product power are plotted in Fig. 4, as a function of input power per tone. The measured results are in good agreement with the predicted values. As the power level is increased the measured IM_3 deviates from the predicted results, because of contributions to IM_3 from higher order distortion products. The frequency dependence of the IM_3 for various input power levels is plotted in Fig. 5. The distortion is observed to be a maximum at the frequency where power transfer from the device to the output circuit is maximum. When the gate bias voltage was made more negative both the gain and the IM_3 were reduced.

Conclusions

An analysis technique has been presented to accurately predict the third-order intermodulation distortion performance of microwave GaAs MESFET amplifiers. Good agreement obtained between the measured and predicted results demonstrates the validity of the model and the accuracy of the analysis technique.

Acknowledgements

This work was supported in part by the Natural Sciences and Engineering Research Council of Canada under Grant NSERC A-3725. The authors wish to thank Dr. A. Javed of Bell Northern Research for many useful discussions. They also thank Mr. Doug Lind for precise etching of the microstrip circuits. R. Gupta wishes to thank Alberta Government Telephones, for the award of a Centennial Fellowship.

References

1. H. A. Willing, C. Rauscher, and P. de Santis, "A Technique for Predicting Large-Signal Performance of GaAs MESFET", IEEE Transactions on Microwave Theory and Techniques, Vol. MTT-26, pp. 1017-1023, Dec. 1978.
2. Minasian, R. A., "Large Signal GaAs M.E.S.E.T. Model and Distortion Analysis," Electronics letters, 16th March, 1978, Vol. 14, No. 6, pp. 183-185.
3. COMPACT User Manual, version 4.75, Compact engineering, Inc., Palo Altos, Ca., U.S.A.
4. R. A. Pucel, H. A. Haus, and H. Statz, "Signal and Noise Properties of Gallium Arsenide Microwave Field-Effect Transistors", Advances in Electronics, L. Morton Ed., Vol. 38, New York: Academic, 1975, pp. 195-264.
5. George L. Heiter, "Characterization of Nonlinearities in Microwave Devices and Systems", IEEE Transactions on Microwave Theory and Techniques, Vol. MTT-21, pp. 797-805, December 1973.
6. S. Narayanan, "Transistor distortion analysis using volterra series representations", Bell System Technical Journal, pp. 991-1024, May-June 1967.

TABLE 1

Modelled Device parameter values for $V_{DS} = 3.0V$, $V_{GS} = -1.0V$

Parameter	Value	Parameter	Value
L_g	1.28 nH	g_m	34.18 mmho
R_g	1.837 ohm	τ_o	12.9 psec
C_{gs}	0.529 pF	R_o	465.9 ohm
R_i	1.15 ohm	C_o	0.4364 pF
R_s	1.1 ohm	R_d	4.875 ohm
L_s	0.16 nH	L_d	0.663 nH
C_{dg}	0.0514 pF		

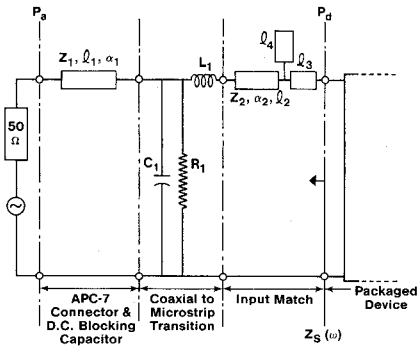


Fig. 1(a) Distributed model for the MESFET amplifier input circuit.

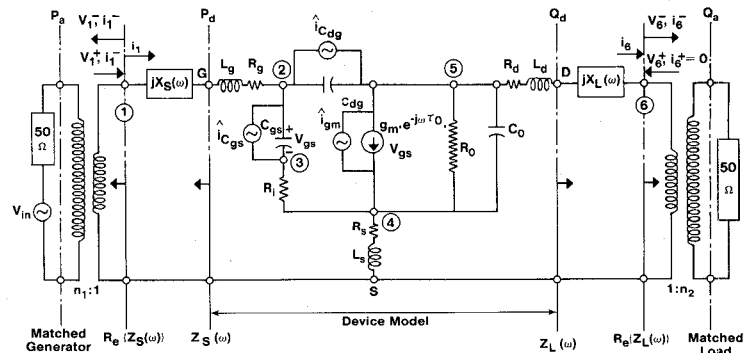


Fig. 1(b) The nonlinear lumped circuit model for the overall amplifier.

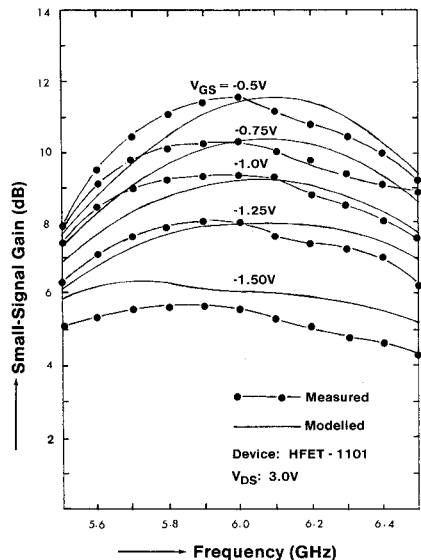


Fig. 2 Dependence of small-signal gain on frequency, for several gate-bias voltages.

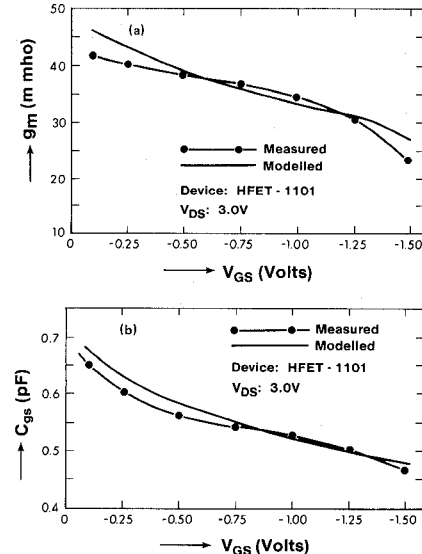


Fig. 3 Comparison of the measured and modelled bias dependence of nonlinear elements.
(a) transconductance
(b) gate-to-source capacitance

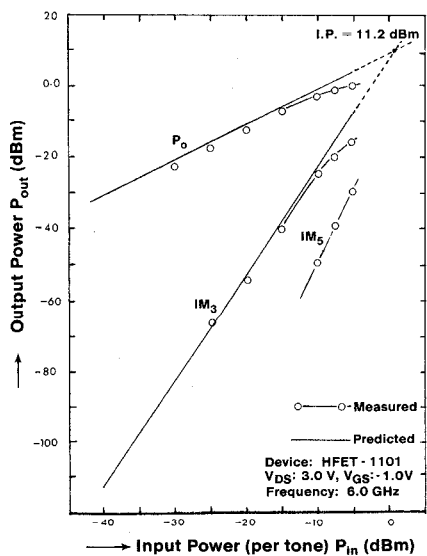


Fig. 4 Dependence of fundamental and intermodulation product output on input power level. (Two equal-amplitude tones: $f_1 = 6.000$ GHz, $f_2 = 6.001$ GHz).

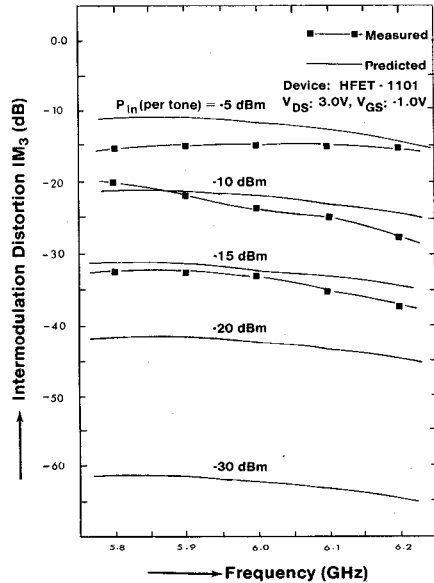


Fig. 5 Dependence of the amplifier's IM3 on the frequency of the two-tone signal, for several input power levels.